APPLIED PHYSICS LETTERS **100**, 263903 (2012)

Temperature dependent conductivity of polycrystalline Cu_2ZnSnS_4 thin films

V. Kosyak,[1] M. A. Karmarkar,[1] and M. A. Scarpulla[1,2,a)]

[1]*Department of Materials Science and Engineering, University of Utah, Salt Lake City, Utah 84112-9206, USA*

[2]*Department of Electrical and Computer Engineering, University of Utah, Salt Lake City, Utah 84112-9206, USA*

(Received 23 March 2012; accepted 11 June 2012; published online 28 June 2012)

The temperature-dependent conductivity of Cu_2ZnSnS_4 (CZTS) thin films prepared by sulfurization of different sputtered ZnS/Cu/Sn stacks and also of the same stack annealed for different times was investigated from 30-300 K. Fitting of the through-thickness conductivity requires a model including Mott variable-range hopping (M-VRH), nearest-neighbor hopping (NNH), and thermionic emission over grain boundary (GB) barriers. The GB barrier height varies sensitively from 50–150 (±5) meV with annealing and especially with [Cu]/([Zn] + [Sn]) ratio but is independent of [Zn]/[Sn] ratio. These results are critical for understanding the behavior of solar cells based on polycrystalline CZTS absorber layers. © *2012 American Institute of Physics*. [http://dx.doi.org/10.1063/1.4731875]

The $Cu_2ZnSn(S,Se)_4$ (CZTSSe) alloy system is a potential alternative material to $Cu(In,Ga)(S,Se)_2$ (CIGSSe) for thin film photovoltaic absorber layers owing to its potential for unconstrained scale-up to >TW production levels based on material availability[1] and the recent demonstration of power conversion efficiencies exceeding 10%.[2] The properties of grain boundaries (GBs) in $CuInS_2$, $CuInSe_2$, and $CuInGaSe_2$ (the CIGSSe alloy system) are fairly well-established[3–6] however the understanding of GBs in CZTS is in its infancy.[7–9] The self-passivation of GB recombination centers by high concentrations of native acceptors at the grain interfaces is typical for CIGSe polycrystalline thin films and is one of the important factors leading to high conversion efficiencies.[4,10,11] Different conduction mechanisms dominate over different temperature ranges in polycrystalline thin film photovoltaic absorber layers.[9,12–17] Typically, thermionic emission (TE) across GBs dominates from room temperature to approximately 150 K and various forms of hopping dominate for $T < 150$ K.[9,12–17] Theoretical studies[18,19] and all experiments to date indicate facile formation of native acceptors in CZTS, which suggests that the possibility of similar self-passivation in this material may be high.[8] However, quantitative comparisons of built-in fields measured at the surface using scanning probe techniques at GBs for CIGSe and CZTS indicate that the magnitudes are similar but slightly lower in CZTS.[7]

In this work, we measure temperature-dependent conductivity (σ(T)) on CZTS thin films and extract the GB barrier magnitudes as well as parameters of hopping conduction at lower temperatures, which probe intragranular transport. Because point defect equilibrium in CZTS is quite complex,[18,19] the details of point defect populations in the bulk and at GBs are very difficult to predict. To date, most studies have focused on developing higher efficiency CZTS photovoltaic cells or structural and optical characterization of the absorber material[20,21] whereas the electrical properties of CZTS layers remain much less studied.[9,22,23] Recent results showing drastically decreasing efficiency and increasing series resistance as temperature is reduced[24,25] demonstrate that understanding the fundamentals of electrical transport in CZTS is of utmost importance.

Photocarrier transport in the depletion region of the CZTS in a working device is different than the transport of majority carriers probed in this work. However, the depletion width may not extend fully through the CZTS layer especially for thicker layers and higher doping. Also, the depletion width will decrease at points on the illuminated I-V curve approaching the open circuit voltage—e.g., at the maximum-power operating point. Thus the measurements in this work will be crucial for understanding the contribution of the CZTS layer outside of the depletion width to a solar cell's series resistance, which is noted as a current issue in CZTS cell technology.[25]

Compositional variation in CZTS affects the populations of shallow dopant and deeper defect levels within grains and at GBs. Details of thermal processing of films during deposition and post annealing are also important to defect populations as well as film microstructure.[26] This study examines the influences of annealing time and chemical composition on the conductivity of CZTS thin films in order to elucidate some of these factors.

Two sets of samples were investigated and are summarized in Table I. The substrate for the annealing time series was 1 mm thick soda-lime glass (SLG) with a 750 nm low-stress Mo layer sputtered in-house while for the composition series, 3 mm thick SLG sputter coated with 275 nm Mo purchased from Saint-Gobain was used. Precursor stacks were radio-frequency (RF) sputtered from ZnS, Cu, and Sn targets. For the annealing time series, a single precursor stack of SLG/Mo/ZnS (360 nm)/Cu (90 nm)/Sn was annealed at 510 °C for 10, 30, 75, and 120 min (samples 10 T, 30 T, 75 T, and 120 T, respectively). The Sn deposition time was empirically optimized, since pure sputtered Sn forms globules.[21] For the composition series, ZnS (240–450 nm), Cu (65–110 nm), and Sn were RF sputter deposited at varying thickness (in that order) with total thickness constant at 1 μm and annealed for 30 min at 510 °C.

a)Author to whom correspondence should be addressed. Electronic mail: scarpulla@eng.utah.edu.

TABLE I. Parameters of the CZTS thin films determined as described in the text.

		Composition ratios from EDX (±2 at. % for EDX)			M-VRH			NNH	TE
Sample	Anneal. time (min)	$\gamma \equiv$ [Cu]/([Zn] + [Sn])	$\delta \equiv$ [Zn]/[Sn]	l (nm) (±20 nm)	T_0 (K) × 10^4	T_0/T (70 K)	E_1(meV) (±0.5 meV)	E_2 (meV) (±2 meV)	E_3 (meV) (±3 meV)
				Composition series (250 nm Mo)					
1C	30	0.90	1.3	117	10.5	1500	9	29	155
2C	30	0.74	1.4	120	5.6	800	4	33	152
3C	30	0.73	1.8	100	10	1430	8	28	150
4C	30	0.61	0.71	100	2.1	300	2	32	112
5C	30	0.63	1.9	103	1.9	271	2	26	107
				Annealing time series (750 nm Mo)					
120 T	120	0.90	1.4	194	13	1860	9	27	112
75 T	75	0.89	1.4	116	6.4	914	5	26	70
30 T	30	0.90	1.4	214	2.4	335	2	26	66
10 T	10	0.89	1.4	200	2.7	379	2	20	48

We have employed a small-volume quartz annealing chamber with low thermal mass capable of high ramp rate of greater than 10 °C/min. Loss of volatile species from the film by re-evaporation was avoided as per Ref. 27 with fast ramp rates[28–30] and by supplying elemental powdered S and metallic Sn inside a closed graphite box with the sample. All samples for this paper were annealed at 510 °C and in forming gas (4% H_2) atmosphere at 2 atm pressure.

Samples surface morphology, grain size, and composition were analyzed in a FEI Quanta 600FEG scanning electron microscope (SEM) equipped with energy dispersive x-ray spectroscopy (EDX). All samples in the annealing time series were Cu-poor ($\gamma \equiv$ [Cu]/([Zn] + [Sn]) = 0.9) and Zn-rich ($\delta \equiv$ [Zn]/[Sn] = 1.4) with no experimentally significant changes in metal ratios measured after annealing. Sample 1C and the samples in the annealing time series have compositions close to the typical Cu-poor, Zn-rich conditions ($\gamma = 0.74$–0.82 and $\delta = 1.2$–1.3) used in absorber layers for record solar cells.[25] Samples 2C and 3C are Cu-poor ($\gamma = 0.74$ and 0.73) but with varying Zn-richness ($\delta = 1.4$ and 1.8). Samples 4C and 5C are more Cu-poor ($\gamma = 0.63$ and 0.61 but are Sn-rich and Zn-rich, respectively ($\delta = 0.71$ and 1.9). Figures S1 and S2 in supplemental material[31] show SEM images. Average grain sizes were determined by measuring many grains in random directions from multiple image locations using special software.[31] Cross-sectional images at cleaved edges showed equiaxed grains throughout the cross-section. Raman spectroscopy was performed in a Witec AlphaSNOM confocal microscope with 532 nm laser excitation at approximately.

Immediately after etching in 5% KCN solution for 2 min, multiple Au contacts (100 nm thickness and 0.5 mm diameter) were sputtered onto each p-type CZTS film. For conductivity measurements, Au wires were secured to the Au contacts with conductive silver epoxy and samples were held in a closed-cycle cryostat and the through-thickness conductivity of the Mo/CZTS/Au stacks (which is more relevant for photocurrent collection in CZTS photovoltaic cells than the planar conductivity) was measured versus temperature. We tested the temperature-dependent resistivity of the Ag paste itself and found that it was completely insignificant compared to the dependence from the sample.

Fig. 1 displays representative Raman spectra taken from the two sample series which all show the typical CZTS peak structure with A_1 peak at 336 cm^{-1} (336–339 cm^{-1} in literature) having a large shoulder to higher wavenumber and minor peak at 286 cm^{-1}.[29,32] The difference from generally quoted value of A_1 peak at 338 cm^{-1} could be due to unresolved mixture of kesterite and stannite structures or due to strain in the films. Though neither Raman nor x-ray

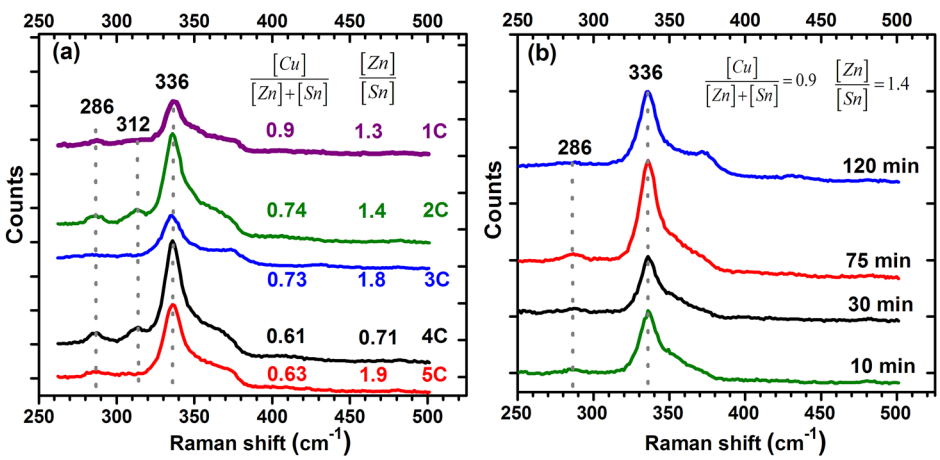

FIG. 1. Raman spectra of the (a) composition series and (b) annealing time series.

diffraction (data not shown) detected Cu_2S in any sample, the Sn-rich sample (4C) and one which is slightly rich Zn (2C) both exhibit a SnS_2 Raman peak at 312 cm^{-1} even after KCN etching. The origin of this peak is discussed in the supplemental material;[31] briefly, SnS_2 surface precipitates are found on the composition series samples because of their degree of Cu-poorness. These SnS_2 platelets project outwards from the CZTS film surface and are not incorporated into the films. Because of the large exposed CZTS surface area, the films' surface roughness, and the similarity of the conductivity activation energies between the two series of samples, we discount the possibility that their presence significantly modifies the conductivity data presented herein. For the annealing time series, Raman characterization indicates that CZTS forms by 10 min of annealing at 510 °C with phonon mean free path (presumably limited by grain size per the data in Table I) increasing slightly with longer annealing. This is evidenced by the reduction in full width half maximum of the A_1 peak from 19 cm^{-1} to 17 cm^{-1} for the 10 T and 75 T samples.

Fig. 2 shows σ(T) data sets for the same samples from Fig. 1 as well as fits to Eq. (1)

$$\sigma = \sigma_{01}\exp\left(\left(-\frac{T_0}{T}\right)^{1/4}\right) + \sigma_{02}\exp\left(-\frac{E_2}{k_bT}\right) + \frac{\sigma_{03}}{T^{1/2}}\exp\left(-\frac{E_3}{k_bT}\right) \quad (1)$$

in which $\sigma_{01} = 3e^2\nu_{ph}\left(\frac{N_{E_F}}{8\pi\alpha k_bT}\right)^{1/2}$, ν_{ph} is the Debye frequency, $T_0 = \frac{\lambda\alpha^3}{k_bN_{E_F}}$ is the Mott characteristic temperature, N_{E_F} is density of states (DOS) at the Fermi energy (E_F), λ is a dimensionless constant, α is the wavefunction decay length, σ_{02} is a constant, E_2 is the nearest neighbor hopping activation energy, σ_{03} is a constant, and E_3 is the GB barrier energy. Equation (1) incorporates (from low to high temperature) Mott variable range hopping (M-VRH), nearest-neighbor hopping (NNH), and TE over GB barriers and well-describes the entire temperature range. We discuss the individual mechanisms below.

We first attempted to fit the $T < 70$ K data with both simple Arrhenius and M-VRH models; better agreement was found with M-VRH. As the values of activation energy E_1 calculated from Arrhenius plot were small ($E_1 < 10$ meV) and $T_0/T \gg 1$ for $T < 70$ K, the hypothesis of M-VRH is self-consistent.[12–17,33] The fitting results are also similar to those from CI(G)Se.[14,17]

According to works,[13–15,34] the Seto model[35] for TE over GB barriers determined only by band bending well-describes the conductivity of polycrystalline films near room temperature. However, studies of CIGSe show that Seto model is not fully adequate—in particular, band gap changes at GBs may exist[4] resulting in several competing GB models.[5,6] Also different scenarios of GB states and doping in the grains predict prefactors with T^0, $T^{-1/2}$, or T^{-1} temperature dependencies which are difficult to distinguish within the current data.[35,36] Because of the lack of data on the bandstructure of CZTS GBs, GB defect states, and intragranular doping, herein we use Seto's formula for TE in the case of partially depleted grains,[35] which has been applied previously to CI(G)Se. This is also the intermediate $\propto T^{-0.5}$ prefactor temperature dependence thus minimizing errors due to model assumptions. The possibility of the high-temperature regime being caused by acceptor freeze-out is discounted as the E_3 energies (a) change with annealing time, (b) do not follow the expected trends with [Cu] and [Zn], which should be associated with the dominant acceptors Cu_{Zn} and V_{Cu} (e.g., smaller activation energies for higher dopant concentrations).[18,37]

Leitao *et al.*[9] assumed that CZTS conductivity at intermediate temperatures is via an admixture M-VRH and TE. However, this is insufficient to explain our data (see Fig. S4 (Ref. 31)), and a third mechanism is necessary in the 50–150 K range. In works (Refs. 38–41), a transition from M-VRH to NNH was seen with increasing temperature. NNH is very plausible in CZTS because of probable high concentrations of native defects.[18,19] The NNH activation energies from 22–33 meV are similar to those for CISe.[42]

The results in Fig. 2 and Table I show that both composition and annealing time result in large changes to both σ(T) and the various activation energies for CZTS thin films. It should be noted that because of the different SLG and Mo thicknesses, we do not directly compare sample 30 T to the composition series despite the identical annealing conditions. By comparing various subgroups of samples, we conclude the following: (1) for the composition series, the GB barrier energy changes from 110 to just over 150 meV as γ increases and is insensitive to δ (including switching from Zn- to Sn-richness); (2) the GB barrier energy increases from 48–112 meV with annealing time from 10–120 min; (3) the

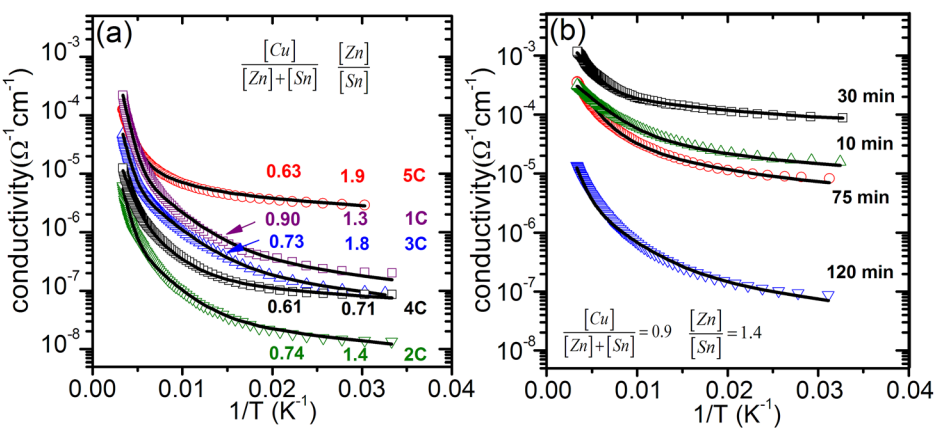

FIG. 2. Temperature dependent conductivity of (a) the composition series and (b) the annealing time series. Experimental data are shown as symbols and fits to Eq. (1) as lines.

NNH activation energy of 20–30 meV varies with overall conductivity and increases slightly with annealing time; (4) for very Cu-poor samples ($\gamma = 0.61$–0.74) annealed for 30 min, the grain size is rather constant near 100 nm irrespective of Sn- or Zn-richness but increases 2 times for $\gamma = 0.9$ for annealing times $\geq$10 min; (5) for $\gamma = 0.61$–0.74, increasing [Zn] (and thus δ) results in overall higher σ(T) but rather constant activation energies for all mechanisms (2C vs. 3C and 4C vs. 5C); and (6) sample 1C with the typical chemical composition for the record efficiency solar cells cell has the highest room-temperature conductivity in the composition series.

With regards to finding (1), the increase of GB activation energy with increased γ (e.g., samples 2C and 3C vs. 4C and 5C) may be explained by the reduction in $[V_{Cu}]$, which may also account for the accompanying decreased T_0. The M-VRH T_0 parameter is inversely proportional to the DOS at the E_F, therefore larger T_0 indicates fewer states near E_F which is consistent with lower $[V_{Cu}]$ (believed to have a small activation energy near 20 meV).[18] Large $[V_{Cu}]$ may passivate GBs electronic states thus decreasing the GB potential barrier. The insensitivity of the GB barrier height to δ (at least in these very Cu-poor films) tends to suggest that Zn- and Sn-related point defects are insignificant both as defects in the GBs and as intragranular dopants.

To explain findings (2) and (3), we hypothesize that longer annealing times lead to diffusion-mediated defect reactions which act primarily to reduce the densities of intragranular acceptor and trap states near E_F. A less significant increasing trend is also seen in the NNH E_2 values. We note that the M-VRH T_0 and E_1 also increase with annealing time indicating that the DOS of localized states near E_F is decreased. The NNH energy E_2 is also inversely related to the overall DOS near E_F which may be modified by acceptors as well as the potentials of compensating donors.[33] We speculate that improvements in crystalline perfection within grains as evidenced by the slight narrowing of the A_1 Raman mode and Na passivation of acceptors such as V_{Cu} may play roles in decreasing the number of electronic states within the grains. Reduction of the density of GB states would actually have the opposite effect of lowering the GB barriers (E_3).

With regards to finding (4) it is well-established in CIGSe and CZTS that larger grains result from higher [Cu] via a fluxing mechanism.[23,29] We also note that the grain size was insensitive to annealing time beyond 10 min.

Regarding conclusion (5), the increase in conductivity for the more Zn-rich 5C over 4C and similarly 3C over 2C may be caused by larger $[Zn_{Sn}]$ (the formation enthalpy of this acceptor is comparatively low).[18] Also, the lower conductivity of 4C compared to 5C may be explained by high [Sn], which may promote compensating Sn_{Zn} donors. We observe generally that increasing γ leads to larger GB barriers while increasing δ leads to overall higher conductivity. This coincides with optimal growth condition for CZTS absorber layers and may contribute to higher cell performance.[25]

Observation (6) that sample 1C has the highest room temperature conductivity is consistent with reducing series resistance in record cells, but is difficult to explain. The reduction of $[V_{Cu}]$ would be inconsistent with increased conductivity because V_{Cu} is expected to be the shallowest acceptor. We also observe that the grain size is essentially the same as for other samples and that the A_1 Raman peak is less-well defined. Thus, we do not expect that the microstructural effects on mobility are significantly lower. We hypothesize that the concentration of the Cu_{Zn} acceptor, which is expected to have very low formation enthalpy even under Cu-poor conditions,[18,19] may be higher. This could lead to the formation of neutral Cu_{Zn}–Zn_{Cu} complexes, which would reduce the ionized impurity scattering and thus increase the mobility.

In conclusion, we analyze temperature dependent conductivity in CZTS thin films using a model including Mott variable-range hopping (M-VRH), nearest-neighbor hopping, and thermionic emission over grain boundary barriers. The behaviors of the overall conductivity and the activation energies for these conduction mechanisms were investigated as functions of composition and annealing time. Perhaps the most important findings are that the grain boundary barrier height is sensitive only to $\gamma \equiv [\text{Cu}]/([\text{Zn}]+[\text{Sn}])$ and not to $\delta \equiv [\text{Zn}]/[\text{Sn}]$ for very Cu-poor films and that it increases monotonically with annealing time for slightly Cu-poor films ($\gamma = 0.9$) due to passivation of intragranular states. While we speculate as to the mechanisms underlying these phenomena, further investigation is warranted to unambiguously identify them as well as the causes of the other observed trends.

We thank A. Bhatia, J. Stoker, and Dr. L. Grenet for invaluable experimental assistance. This work was supported in full by the U.S. Department of Energy, Office of Basic Energy Sciences, Division of Materials Sciences and Engineering under Award DE-SC0001630.

[1]V. Fthenakis, Renewable Sustainable Energy Rev. **13**, 2746 (2009).
[2]D. R. Barkhouse, O. Gunawan, T. Gokmen, T. K. Todorov, and D. B. Mitzi, Prog. Photovoltaics **20**, 6 (2011).
[3]U. Rau, K. Taretto, and S. Siebentritt, Appl. Phys. A **96**, 221 (2009).
[4]M. Gloeckler, J. R. Sites, and W. K. Metzger, J. Appl. Phys. **98**, 113704 (2005).
[5]C. Persson and A. Zunger, Phys. Rev. Lett. **91**, 26 (2003).
[6]Y. Yan, C.-S. Jiang, R. Noufi, S.-H. Wei, H. R. Moutinho, and M. M. Al-Jassim, Phys. Rev. Lett. **99**, 235504 (2007).
[7]J. B. Li, V. Chawla, and B. Clemens, Adv. Mater. **24**, 720–723 (2012).
[8]M. J. Romero, H. Du, G. Teeter, Y. Yan, and M. M. Al-Jassim, Phys. Rev. B **84**, 165324 (2011).
[9]J. P. Leitao, N. M. Santos, P. A. Fernandes, and P. M. P. Salome, Phys. Rev. B **87**, 024120 (2011).
[10]K. Taretto and U. Rau, J. Appl. Phys. **103**, 094523 (2008).
[11]Y. Yan, K. M. Jones, C. S. Jiang, X. Z. Wu, R. Noufi, and M. M. Al-Jassim, Physica B **401–402**, 25 (2007).
[12]S. Siebentritt and S. Schuler, J. Phys. Chem. Solids **64**, 1621 (2003).
[13]A. Amara, W. Rezaiki, A. Ferdi, A. Hendaoui, A. Drici, M. Gueriounea, J. C. Bernede, and M. Morsli, Sol. Energy Mater. Sol. Cells **91**, 1916 (2007).
[14]A. Amara, A. Ferdi, A. Drici, J. C. Bernede, M. Morsli, and M. Gueriоune, Catal. Today **113**, 251 (2006).
[15]R. Caballero and C. Guillen, Thin Solid Films **431–432**, 200 (2003).
[16]M. Nouiri, K. Djessas, J. L. Gauffier, L. E. Mir, and S. Alaya, Thin Solid Films **516**, 708 (2008).
[17]S. Agilan, D. Mangalaraj, Sa. K. Narayandass, G. M. Rao, and S. Velumani, Vacuum **84**, 1220 (2010).
[18]S. Chen, J.-H. Yang, X. G. Gong, A. Walsh, and S.-H. Wei, Phys. Rev. B **81**, 245204 (2010).
[19]A. Nagoya, R. Asahi, R. Wahl, and G. Kresse, Phys. Rev. B **81**, 113202 (2010).
[20]P. A. Fernandes, P. M. P. Salome, A. F. da Cunha, and B.-A. Schubert, Thin Solid Films **519**, 7382 (2010).

[21]H. Katagiri, K. Jimbo, and W. S. Ma, Thin Solid Films **517**, 2455 (2009).
[22]P. M. P. Salome, J. Malaquias, P. A. Fernandes, and M. S. Ferreira, Sol. Energy Mater. Sol. Cells **95**, 3482 (2011).
[23]T. Tanaka, A. Yoshida, D. Saiki, K. Saito, Q. Guo, M. Nishio, and T. Yamaguchi, Thin Solid Films **518**, S29 (2010).
[24]A. Redinger, D. M. Berg, P. J. Dale, R. Djemour, L. Gutay, T. Eisenbarth, N. Valle, and S. Siebentritt, IEEE J. Photovolt. **1**, 200 (2011).
[25]D. B. Mitzi, O. Gunawan, T. K. Todorov, K. Wang, and S. Guha, Sol. Energy Mater. Sol. Cells **95**, 1421 (2011).
[26]H. Nukala, J. L. Johnson, A. Bhatia, E. A. Lund, W. M. Hlaing Oo, M. M. Nowell, L. W. Rieth, and M. A. Scarpulla in *Proceedings of the Material Research Society Symposium, San Francisco, USA* (MRS, 2010), p. EE03-04.
[27]J. Johnson, H. Nukala, E. A. Lund, W. M. Hlaing Oo, A. Bhatia, L. W. Rieth, and M. A. Scarpulla, in *Proceedings of the Material Research Society Symposium, San Francisco, USA* (MRS, 2010), p. EE03-03.
[28]X. Wang, S. S. Li, W. K. Kim, S. Yoon, V. Craciun, J. M. Howard, S. Easwaran, O. Manasreh, O. D. Crisalle, and T. J. Anderson, Sol. Energy Mater. Sol. Cells **90**, 2855 (2006).
[29]J. Scragg, *Copper Zinc Tin Sulfide Thin Films for Photovoltaics, Synthesis and Characterisation by Electrochemical Methods* (Springer Theses, Berlin, 2011), p. 144.
[30]W. M. Hlaing Oo, J. L. Johnson, A. Bhatia, E. A. Lund, M. M. Nowell, and M. A. Scarpulla, J. Electron. Mater. **40**, 2214 (2011).
[31]See supplementary material at http://dx.doi.org/10.1063/1.4731875 for SEM images of the samples, I-V curve and example of fitting results with the 2-regime conductivity model, information about grain size calculation, as well as for some discussion of Raman spectra.
[32]A. J. Cheng, M. Manno, A. Khare, S. A. Campbell, and E. S. Aydil, Vac. Sci. Technol. **29**(5), 051203 (2011).
[33]N. F. Mott and E. A. Davis, *Electronic Processes in Non-crystalline Materials* (Clarendon, Oxford, 1971), p. 590.
[34]S. M. F. Hasan, M. A. Subhan, and Kh. M. Mannan, Opt. Mater. **14**, 329 (2000).
[35]J. Y. W. Seto, J. Appl. Phys. **46**, 5247 (1975).
[36]A. Broniatowski, in *Polycrystalline Semiconductors*, edited by G. Harbeke (Springer, Berlin 1985), Vol. 57, pp. 95–117.
[37]E. F. Schubert, *Doping in III-V Semiconductors* (Cambridge University Press, Cambridge, 1993), p. 628.
[38]N. Brilis, D. Tsamakis, H. Ali, S. Krishnamoorthy, and A. A. Iliadis, Thin Solid Films **516**, 4226 (2008).
[39]D. C. Look, D. C. Reynolds, W. Kim, O. Aktas, A. Botchkarev, A. Salvador, and H. Morkoc, J. Appl. Phys. **80**, 2960 (1996).
[40]C.-C. Lien, C.-Y. Wu, Z.-Q. Li, and J.-J. Lin, J. Appl. Phys. **110**, 063706 (2011).
[41]J. Han, M. Shen, W. Cao, A. M. R. Senos, and P. Q. Mantas, Appl. Phys. Lett. **82**, 67 (2003).
[42]S. M. Wasim, C. Rincon, G. Marin, and R. Marquez, J. Phys. Chem. Solids **64**, 1627 (2003).